Biomedical Microdevices (2018) 20:41
https://doi.org/10.1007/s10544-018-0284-6

A bead-based immunogold-silver staining assay on capillary-driven microfluidics

Ngoc M. Pham[1] · Sebastian Rusch[2,3,4] · Yuksel Temiz[5] · Robert D. Lovchik[5] · Hans-Peter Beck[2,3] · Walter Karlen[1] · Emmanuel Delamarche[5]

Abstract
Point-of-care (POC) diagnostics are critically needed for the detection of infectious diseases, particularly in remote settings where accurate and appropriate diagnosis can save lives. However, it is difficult to implement immunoassays, and specifically immunoassays relying on signal amplification using silver staining, into POC diagnostic devices. Effective immobilization of antibodies in such devices is another challenge. Here, we present strategies for immobilizing capture antibodies (cAbs) in capillary-driven microfluidic chips and implementing a gold-catalyzed silver staining reaction. We illustrate these strategies using a species/anti-species immunoassay and the capillary assembly of fluorescent microbeads functionalized with cAbs in "bead lanes", which are engraved in microfluidic chips. The microfluidic chips are fabricated in silicon (Si) and sealed with a dry film resist. Rabbit IgG antibodies in samples are captured on the beads and bound by detection antibodies (dAbs) conjugated to gold nanoparticles. The gold nanoparticles catalyze the formation of a metallic film of silver, which attenuates fluorescence from the beads in an analyte-concentration dependent manner. The performance of these immunoassays was found comparable to that of assays performed in 96 well microtiter plates using "classical" enzyme-linked immunosorbent assay (ELISA). The proof-of-concept method developed here can detect 24.6 ng mL^{-1} of rabbit IgG antibodies in PBS within 20 min, in comparison to 17.1 ng mL^{-1} of the same antibodies using a ~140-min-long ELISA protocol. Furthermore, the concept presented here is flexible and necessitate volumes of samples and reagents in the range of just a few microliters.

Keywords Microfluidics · Silver staining · Immunoassays · Microbeads

1 Introduction

Healthcare facilities in the developing world consist not only of centralised laboratories in well-equipped hospitals in cities, but also of primary healthcare centres with limited infrastructure in peripheral regions. In such settings, POC diagnostics are critical for guiding appropriate treatments for infectious diseases such as malaria, in which the delay between diagnosis and treatment can be life threatening (Peeling and Mabey 2010). Developments of innovative technologies has transformed POC diagnostics to bring healthcare services closer to patients (BIO Ventures for Global Health 2010). There are many benefits that well reflect this transformation, for example the increasing number of rapid antigen detecting tests, or POC immunodiagnostic assays for malaria and HIV (UNITAID 2017, 2016). There are two main diagnostic platforms that are being used for POC applications: conventional lateral flow assay technology and emerging microfluidics-based technologies (Sharma et al. 2015). While the lateral flow technology has a long history with a number of successful stories in commercialising diagnostic products, there are only very few microfluidics-based tests available in the market (Chin et al. 2012).

Sensitive detection and simplicity of use are prerequisites for POC diagnostic assays (Yager et al. 2006). In other words, compelling performance and affordability are current

✉ Emmanuel Delamarche
emd@zurich.ibm.com

1 ETH Zürich, Mobile Health Systems Lab, Institute for Robotics and Intelligent Systems, Department of Health Sciences and Technology, BAA, Lengghalde 5, 8092 Zürich, Switzerland

2 Swiss Tropical and Public Health Institute, Socinstrasse 57, 4051 Basel, Switzerland

3 University of Basel, Petersgraben 1, 4001 Basel, Switzerland

4 Present address: Kantonsspital Aarau AG, Institut für Labormedizin, Medizinische Genetik, Tellstrasse 25, CH-5001 Aarau, Switzerland

5 IBM Research – Zurich, Säumerstrasse 4, CH-8803 Rüschlikon, Switzerland

Published online: 21 May 2018

challenges for microfluidics-based diagnostic chips (Chin et al. 2012). Fluorescence, luminescence and absorbance are three optical detection methods that have been implemented for signal transduction of the immunobinding reactions in low cost, microfluidics-based POC diagnostics (Baker et al. 2009; Gai et al. 2011; Kuswandi et al. 2007). Fluorescence-based assays offer high sensitivity and selectivity (Lin et al. 2011). Such immunoassays rely on fluorophores that are linked to detection antibodies (dAb) and that can emit a fluorescence signal upon excitation using a specific wavelength. The intensity of the fluorescence signal is proportional to the amount of antigens selectively captured on a surface. Organic fluorescent dyes and quantum dots are commonly used as labels. For example, an ultrasensitive fluorescence immunoassay was developed to simultaneously detect two cancer biomarkers, carcinoma embryonic antigen and α-fetoprotein, in serum using CdTe/Cds quantum dots as fluorescent probes (Hu et al. 2010). The limit of detection (LOD) of this fluorescence immunoassay on the microfluidic chips was 250 femtomolar, which is 3 orders of magnitude better than that of assays using conventional fluorescence probes. Issues that are hindering further progress on fluorescence-based POC diagnostics are the (photo)stability of fluorophores and the cost, complexity and fragility of fluorescence readers. Luminescence is a method used in variants of standard immunosorbent assays. In luminescence immunoassays, an enzyme conjugated to the dAb converts a substrate into a product that emits light (Mirasoli et al. 2014). Unlike fluorescence, this method does not require an optical excitation source, therefore luminescence detection is simpler than that of fluorescence in terms of optics. In a recent example showing the implementation of this technique in a portable and microfluidics-based diagnostic platform, a chemiluminescent assay detecting C-reactive protein (CRP), a biomarker that indicates inflammation in the body when its concentration exceeds 5 μg mL^{-1}, was developed (Hu et al. 2017). In this prototype, the LOD for CRP reached 4.27 ng mL^{-1}, which is comparable to conventional chemiluminescent immunoassays in laboratories. Furthermore, the compact design of this prototype with all-integrated reagents and pre-programmed on-chip mechanical valves for controlling the steps of the assay showed the technical feasibility of implementing a luminescence assay into a POC platform. Nevertheless, the stability and cost of the enzyme used for such assays need to be addressed. Hydrogen peroxide or chemicals that are needed for chemiluminescence are unstable at ambient conditions and require storage at low temperatures, which is also cumbersome for the development of fully integrated POC diagnostic devices.

Perhaps the most popular detection method used in commercially-available diagnostic immunoassays is the one based on absorbance detection. Absorbance-based assays rely on the conversion of a substrate into a strongly coloured product by an enzyme, which is linked to a dAb (Novo et al. 2011). Although being slightly less sensitive than fluorescence- and luminescence-based immunoassays, these assays offer a reasonable performance and can involve relatively low cost reagents and chemicals (Shekarchi et al. 1985; Yu et al. 2011). To improve the performance of assays using absorbance measurements, metal nanoparticles (NPs) such as gold NPs are used to intensify colorimetric signals of assays (Xu et al. 2009). Typically, the size of gold NPs varies from 10 to 50 nm (Sun et al. 2014). Larger gold NPs might create steric hindrance for ligand-receptor interactions and smaller gold NPs can be challenging to visualize (Liu et al. 2014). Holgate et al. proposed to use immunogold silver staining (IGSS) to solve this problem by depositing silver on the surface of gold NPs to enhance the signal intensity after the ligand-receptor binding has taken place (Holgate et al. 1983). To investigate the suitability of IGSS for diagnostic assays, a lateral flow assay for influenza was engineered, detecting hemagglutinin of H5-type of influenza viruses (Wada et al. 2011). LOD of the silver amplified assay was decreased 500 times compared to that of the assay without silver amplification, and this LOD was 10 times lower than that of commercial influenza rapid diagnostic tests. Similarly, the IGSS method was used to detect HIV and rubella infections in blood samples and the LODs were comparable to the reference methods (Patel et al. 1991; Rocks et al. 1991). The specificity of both assays using IGSS was also higher and interferences due to cellular components of whole blood specimens were less prominent than with other commonly used diagnostic methods.

In this paper, we present a capillary-driven microfluidic chip for IGSS with capture antibodies (cAbs) for analytes located on the surface of microbeads. We specifically developed an assay using species and anti-species polyclonal antibodies to demonstrate how such assay can be implemented. There are three key features in this approach. First, the beads are self-assembled from a bead suspension into specific structures of the chip and the chip is sealed by lamination with a dry film resist (DFR) layer at low temperature. This makes the integration of beads and biological receptors into the microfluidic chip simple, fast and versatile. Second, the core of the beads is fluorescent and the growth of a metallic silver layer during the silver staining step efficiently attenuates/quenches this fluorescence, which also eliminates the need for fully transparent microfluidic devices for measuring absorption of light by the formed silver film. The fluorescence signals are extremely strong when no analyte is present in the sample and fluorescent beads are highly stable against photobleaching. Third, the microfluidic chip is designed to accommodate sub-microliters of solutions, which are sequentially pipetted for the IGSS assay. All handling steps for the assay take as little as 20 min and there is no need for active microfluidic elements to perform the assay.

2 Materials and methods

2.1 Antibodies and reagents

All reagents were purchased from Sigma-Aldrich unless otherwise stated. Water was purified using a Simplicity 185 system (Millipore, Billerica, MA). Phosphate buffered saline (PBS) solution was prepared by dissolving commercially available PBS tablets. A solution of 1% *w*/*v* bovine serum albumin (BSA) was prepared in PBS. PBS with Tween 20 (PBST) was prepared by adding Tween 20 to PBS to a resulting concentration of 1%. 3,3′-5,5′-tetramethylbenzidine in water (BM Blue POD substrate) was used as a substrate for enzyme-based immunoassays. A 1:1 *v*/v mixture of silver A and silver B from SE 100–1 KT silver enhancer kit was prepared prior to the signal amplification step. Streptavidin-coated 96-well microtiter plates and blocker BSA solution were from Life Technologies. Fluorescent streptavidin PMMA beads (PolyAn GmbH, Red 25, 5.9 μm diameter) were used as carriers to integrate the cAb in microfluidic chips. Biotinylated anti-rabbit IgGs was used as cAb. Donkey anti-rabbit IgGs conjugated with 6 nm gold nanoparticles (abcam) and donkey anti-rabbit IgG conjugated with horseradish peroxidase (HRP) (abcam) were used as dAbs. Rabbit IgGs and mouse IgGs were used for positive and negative control experiments for immunoassays on 96-well microtiter plates.

2.2 Fabrication materials

Si wafer (Si-Mat, Kaufering, Germany) and SU-8 photoresist (SU-8 3010, MicroChem Corp.) were used to fabricate microfluidic chips. Acetone and isopropyl alcohol were used to clean the microfluidic chips after dicing. DFR (DF-1050, Engineered Materials Systems, Inc., USA) was used to seal the chip.

2.3 Protocols for assays

To validate the reagents and characterize the assay protocol, the IGSS assay was first performed using standard streptavidin-coated 96-well microtiter plates. Between each step, the plates were washed three times using a plate washer (Tecan). First, 50 μL of a biotinylated anti-rabbit IgG solution (10 μg mL^{-1}) was added into each well and incubated for 30 min at room temperature (RT). Then solutions of rabbit IgG (positive control) and mouse IgG (negative control), were added into each well using a serial dilution factor of 2 with the starting concentration 4 μg mL^{-1} in the first wells (50 μL/well). The incubation was 30 min at RT. For silver staining, a solution of gold conjugate was diluted 1:2000 (*v*/v) in 1% BSA in PBST and added into each well (50 μL/well). Incubation of the analyte with dAb-conjugated gold was 15 min at RT. Solutions of silver A and silver B were mixed (1:1, *v*/v) and added immediately into each well (50 μL/well). The silver development step was 20 min, at RT and in the dark (plates covered with an aluminium foil). For standard enzymatic assays, a solution of HRP conjugate was diluted 1:10′000 (*v*/v) in 1% BSA in PBST and added into each well (50 μL/well). This incubation was 60 min at RT. Solutions containing POD blue were added (50 μL/well) and the enzymatic reaction was allowed to proceed for 20 min. To measure the end-point absorbance, a plate reader (Sunrise, Tecan) was used at a wavelength of 570 nm and the absorbance measurements were taken at RT.

For immunoassays performed on microfluidic chips, aliquots of solutions were sequentially added to the loading pads of the chip. Fluorescence images of the beads integrated into the microfluidic chip before and after the silver staining step were taken using a fluorescence microscope (Nikon Eclipse 90i, Japan) equipped with a 20× objective and a Texas Red fluorescence filter. Excitation of fluorophores was done using an LED Lumencor lamp (software SOLA S2 Controller). Images were taken using a black and white CCD camera (DS-1 QM, Nikon) and an acquisition time of 400 ms and using a ND16 filter. The software Fiji (ImageJ) was used to analyse the fluorescence images. Fluorescence images for regions of interest (ROI) comprising the beads before and after silver staining were acquired and the mean fluorescence intensity for each experiment was obtained by subtracting the background signal around an ROI to the mean signal value in the ROI.

3 Results and discussion

3.1 Assay and detection principles

The strategy to implement a silver staining technique for microfluidics-based immunoassays is outlined in Fig. 1. Two steps are performed off-chip, Fig. 1a. First, fluorescent microbeads, which are functionalized with streptavidin, are incubated with biotinylated cAb (1:5 *v*/v). These beads are then integrated into specific microstructures (“bead lanes”) so that the cAbs are localized in a well-defined area of the chip. The sample containing the analytes (antigens) is then mixed with a solution of dAb conjugated to gold nanoparticles for 1 min (1:1 *v*/v). The assay takes place by having this solution passing over the integrated beads, leading to the capture of antigen-dAb complexes by cAb on the beads, Fig. 1b. Gold nanoparticles on the dAb then catalyze the deposition of silver from a staining solution. The formation of this silver metallic film attenuates the emitted fluorescent signal of the beads, which provides optical signal readout. The type and volume of solutions sequentially added to a loading pad of the microfluidic chip are listed in Fig. 1c. Each added solution

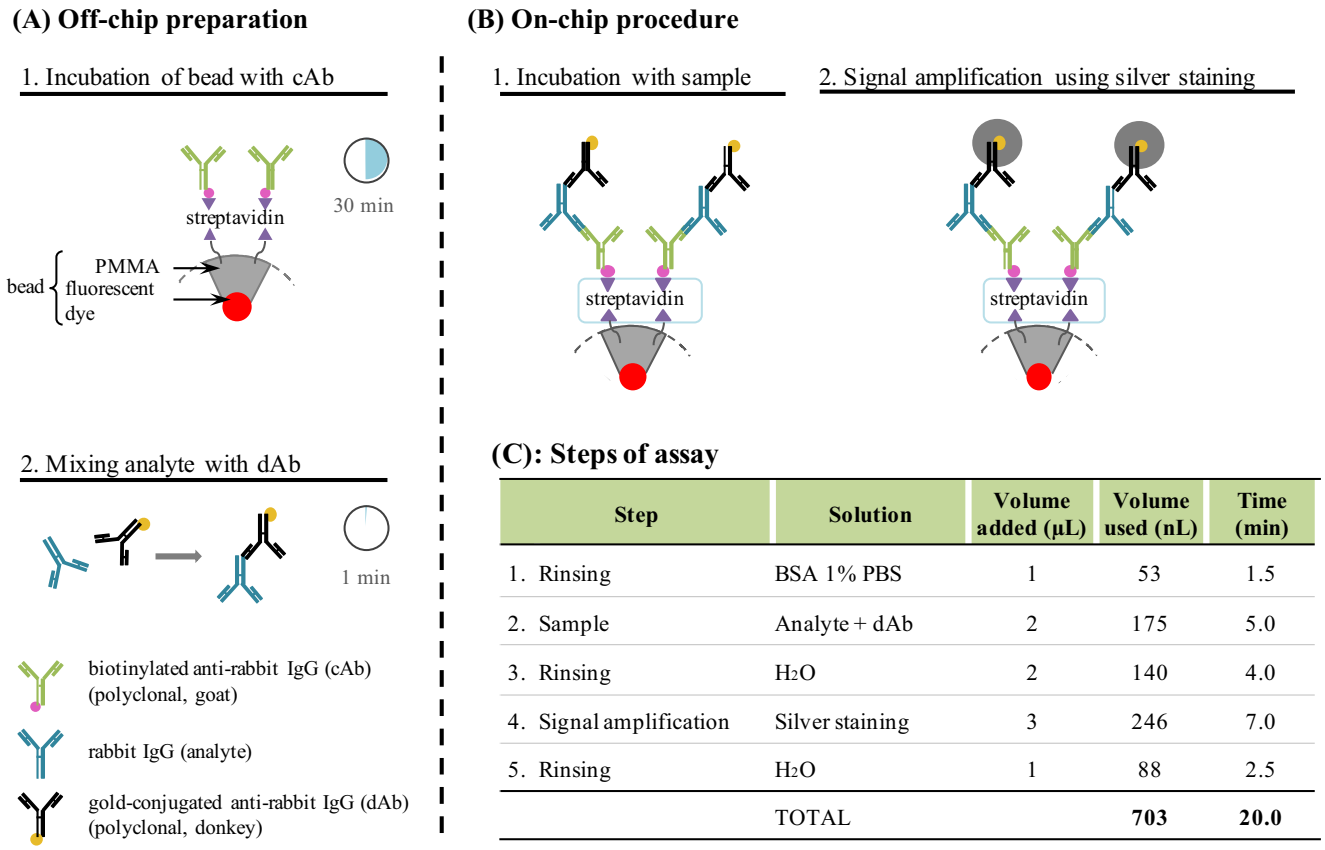

(C): Steps of assay

Step	Solution	Volume added (µL)	Volume used (nL)	Time (min)
1. Rinsing	BSA 1% PBS	1	53	1.5
2. Sample	Analyte + dAb	2	175	5.0
3. Rinsing	H_2O	2	140	4.0
4. Signal amplification	Silver staining	3	246	7.0
5. Rinsing	H_2O	1	88	2.5
	TOTAL		**703**	**20.0**

Fig. 1 Architecture of the IGSS assay implemented using capillary-driven microfluidic chips and beads functionalized with receptors. **a** The off-chip steps comprise of: 1. incubation of streptavidin-coated fluorescent beads with biotinylated cAb for 30 min and 2. mixing of sample (rabbit IgG in BSA1% PBS) with dAb for 1 min to form the complex analyte/dAb before loading the resulting solution to the microfluidic chip. **b** The key steps of the on-chip part of the assay are: 1. the incubation of the analyte/dAb complex with cAb on bead located in the microfluidic chip, and 2. the signal amplification step during which silver staining occurs in presence of gold nanoparticles conjugated to dAb. **c** Summary of the steps involved in the on-chip procedure. Each liquid is allowed to flow for a specific time as indicated

starts to flow in the microfluidic chip owing to capillary action. When the solution has flown for the desired time, the excess solution left in the loading pad is removed using a cleanroom tissue and the next solution is added.

The first added liquid is a 1% solution of BSA in PBS and it is allowed to flow for 1.5 min (i.e. ~53 nL based on optically monitoring the advancement of the solution in the chip) to block surfaces and prevent non-specific adsorption of analytes and dAbs up to the receptor areas. The assay proceeds with the addition of the pre-mixed antigen-dAb solution (1:1 *v*/v), which is allowed to flow for 5 min (~175 nL). The antigen-dAb complex is captured by the cAb present on the beads during this step, Fig. 1b. Then, deionised water is added for a 4-min rinsing step (~140 nL) before adding a silver staining solution, which is allowed to flow for 7 min (~246 nL). In presence of antigens, a film of metallic silver forms on the surface of beads. During this silver staining step, the microfluidic chip is covered with an aluminium foil to avoid non-specific, light-catalysed reduction of silver. The addition of deionised water displaces the silver staining solution where beads are located and stops the formation of the silver film so that the fluorescence emitted from beads can be measured.

3.2 Chip design and bead integration

The microfluidic chip for implementing the IGSS assay is shown in Fig. 2. The chip is approximately 1 cm^2 in size and contains six types of microfluidic elements: anti-wetting structures, 2 loading pads, a flow resistor, 2 bead lanes, a capillary pump, and an air vent, Fig. 2a. All structures are 15 µm deep and defined in a layer of SU-8 with the exception of bead lanes, which are etched in the Si layer itself. These bead lanes accommodate beads functionalized with cAb, Fig. 2b. Each lane can hold approximately 200 beads and the beads are solely present in the bead lanes after their integration to the chip as seen in the SEM image of Fig. 2b. Once a liquid is pipetted onto a loading pad, it follows the microfluidic elements along the flow path owing to capillary action. The flow resistor has the function of slowing down the flow so that sufficient time can be obtained for the binding of analytes to

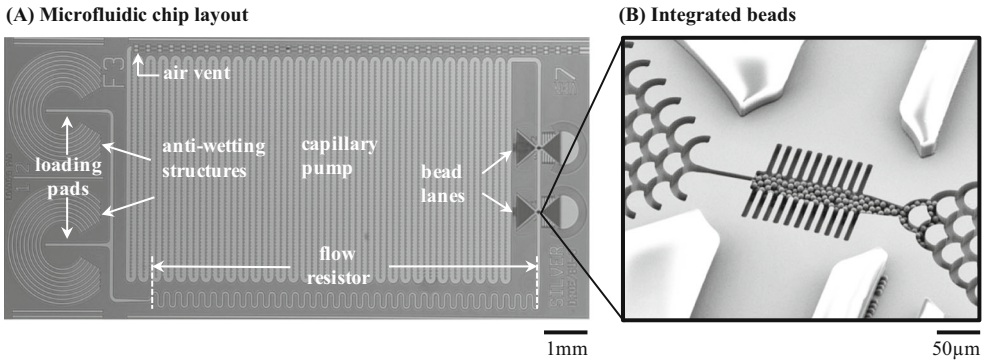

Fig. 2 **a** Photograph of the microfabricated Si microfluidic chip for IGSS immunoassays with the main functional components being indicated: a loading pad surrounded with anti-wetting structures, flow resistor, "bead lanes", capillary pump, and air vent. All microfluidic structures are formed in a 15-µm-high photoresist layer. The chip is 15-mm-long and 6.5-mm-wide (97.5 mm^2). **b** SEM micrograph of a bead lane (15-µm-deep, etched in Si and 20-µm-wide) where beads functionalized with receptors have been supplied from a suspension passing from right to left when the chip surface was still open, which resulted in the retention and packing of beads after the drying of the bead containing solution. The beads are 6 µm in diameter

cAbs on the bead or for the silver staining reaction. Up to 5 µL of liquid can be added to a loading pad and semi-circular ridges around pads act as anti-wetting structures and prevent spreading of the added liquid to the adjacent loading pad or edges of the chip due to liquid pinning. Depending on the desired volume of liquid that needs to enter the flow path, excess of liquid in a loading pad can be readily removed using a cleanroom wiping paper. Volumes of liquids added to the chip are estimated based on the observed flow rates and filling state of the capillary pump. The IGSS assay demonstrated here only requires ~700 nL of sample and reagents. The assay conditions can be adapted by varying the dimensions of the flow resistor and capillary pump, which impact both the flow resistance of the flow path and the capillary pressure along it.

The fabrication steps for making the microfluidic chips are shown in Fig. 3. The fabrication uses standard clean room processes and only two photolithography masks. A low-cost single side polished Si wafer is used as the substrate. First, the

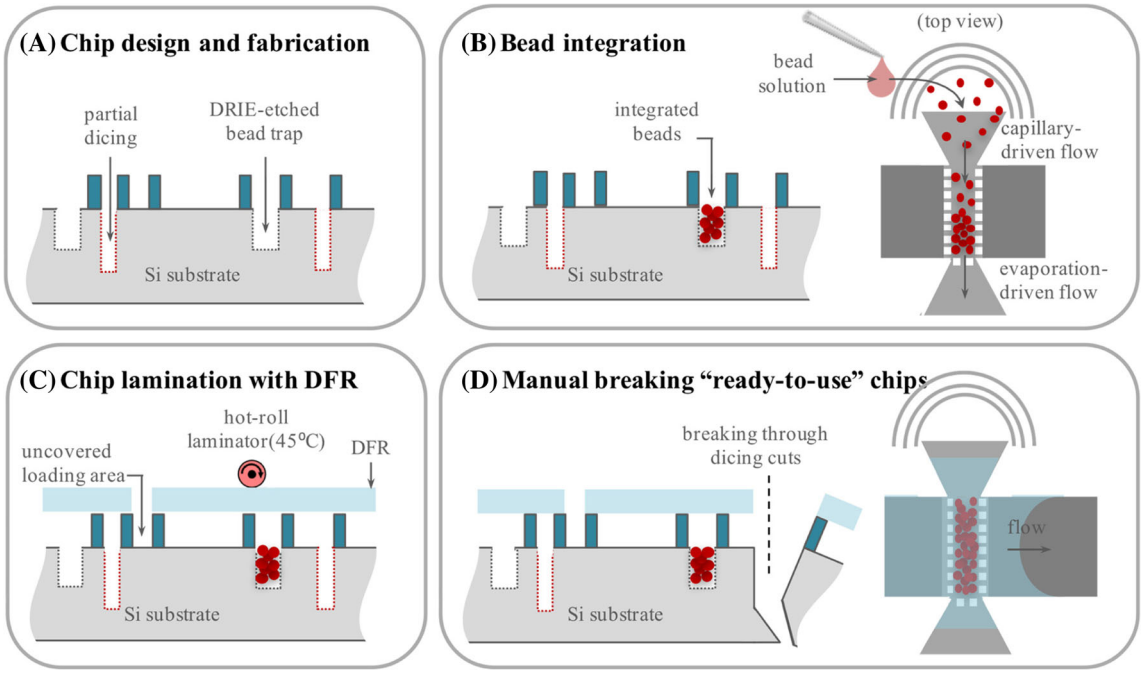

Fig. 3 Main fabrication steps of the microfluidic chips. **a** Two lithographic masks are used to define 15-µm-high structures in SU-8 (microfluidic path) and 15-µm-deep structures in Si to form bead lanes. Once the lithographic steps are done, the wafers are partially diced. **b** A suspension of beads functionalized with receptors is pipetted to a pad connected to the bead lane. Beads accumulate and pack in the bead lane during drying of the suspension. **c** Microfluidic chips are laminated at low temperature with a stripe of DFR. **d** Single chips are released from the wafer by breaking by hands and are ready to use. The items in the figure are not drawn to scale and top views of the bead lanes during packing with the beads (**b**) and flow of sample across the bead lane (**d**) are provided for clarity

bead lane structures are etched anisotropically to a depth of 15 μm using deep reactive-ion etching (DRIE) and a 1.2 μm positive-tone photoresist as the masking layer. This etching step takes only 3 min per wafer and feature sizes as small as 2 μm can be patterned without any optimization. Based on preliminary experiments for integrating beads using different channel depths for the bead lanes, a minimum channel depth of 10 μm creates enough capillary pressure to completely wet the bead lane when the top surface is still open. Following the Si etching step, a 15 μm-thick SU-8 layer is patterned for the microfluidic structures using the recipe provided by the supplier. The presence of the etched bead lanes does not adversely affect the uniformity of the spin-coated SU-8 layer because the bead lanes occupy less than 2% of the total chip area. The wafer is then diced to half of its thickness using a semi-automated dicing tool to define individual chips. The partially diced wafer is immersed into acetone then rinsed in isopropyl alcohol to clean the surface for the bead integration step.

The bead integration step is initially facilitated by capillary actions followed by evaporation of carrier solution, Fig. 3b. 0.5 μL bead solution in 1% BSA in PBST (0.01%) (0.5% *w*/*v*) is introduced at the bead loading pad when the chip surface is still open. Bead solution flows orthogonal to the main channel and only beads are trapped at the bead lane. More bead solution can be loaded if needed until the bead lane is completely filled with beads. Lateral spreading of the excess liquid in the main channel is minimized owing to the lower capillary pressure in the main channel compared to the bead lanes. Because the beads self-assembly process happens without using any external energy, many bead lanes can be filled with beads in a short time by serial deposition of the carrier solution. This makes the technique compatible with mass production using automated pin spotters. Following the integration of the beads, the chip surface needs to be sealed to create a strong capillary pressure of samples required for the assay and to minimize evaporation. Many sealing techniques are available for microfluidic applications, such as adhesive or thermal bonding. However, these techniques are typically not compatible with integrated reagents because of the use of solvents and/or high temperatures. Here, the sealing of the chip is performed by gently laminating a 50-μm-thick DFR at 45 °C. This low temperature and fast (<10 s) sealing process ensures proteins coated on the bead surface are minimally affected, Fig. 3c. In addition, it is not required to structure the DFR to pattern the openings for the loading pads. A straight cut aligned to the loading pads is sufficient to hold the pipetted liquid owing to the anti-wetting structures. Because all channel walls are inherently hydrophilic, no additional surface treatment is needed for the capillary flow. Finally, ready-to-use chips can be singulated by manual breaking through the partially diced regions, Fig. 3d (Temiz and Delamarche 2014). This step also breaks the DFR, making the whole process compatible with wafer-level reagent integration and sealing. For a standard clean room using 200 mm Si wafers, this process would yield more than 300 chips per wafer.

3.3 Assay implementation validation

ELISAs are very well-established assays and therefore can be used as a gold standard to evaluate microfluidics-based immunodiagnostic assays. We compared the sensitivity between IGSS and ELISA carried out on microtiter plates using a bench-top plate reader for absorbance measurements. The titration data for both types of assays are fitted using a 4-parameter logistic regression (4-PL) (Fig. 4.) The LOD for these assays is defined as the smallest concentration of analyte for which the signal is above the mean signal +2 standard deviations (95% confidence interval) of samples not containing analytes. For an immunoassay detecting rabbit IgG, the LOD of the IGSS was 17.1 ng mL^{-1}, while the LOD of the

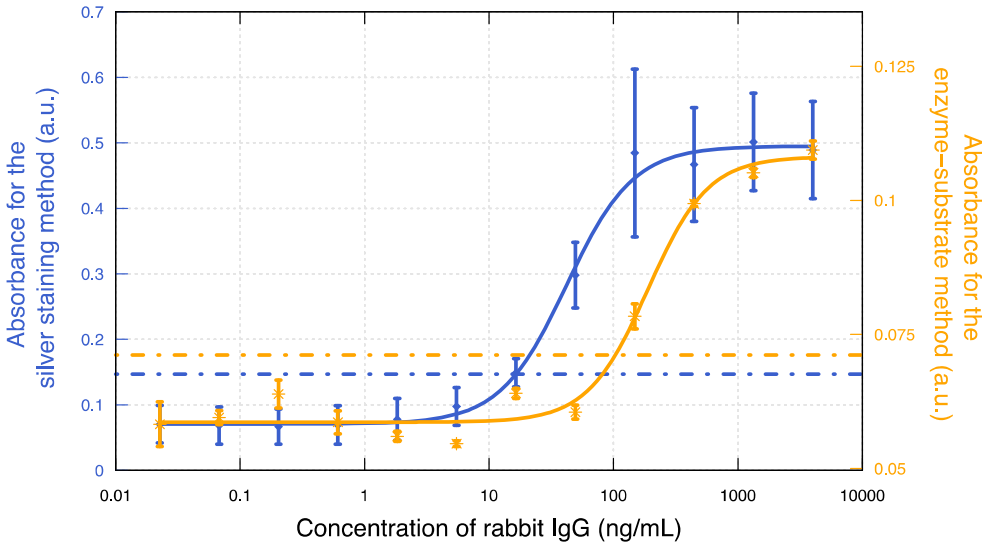

Fig. 4 Comparative absorbance measurement of ELISA and the IGSS immunocapture of rabbit IgGs. Standard deviations correspond to triplicate of experiments and shown as error bars. Dotted lines represent the cut-off values of each method (based on the average values of negative samples and two times the standard deviations)

ELISA was 103.2 ng mL^{-1}. This result indicates that the performance of IGSS is slightly superior to bench-top ELISAs.

With the aim of implementing the IGSS in immunodiagnostic assays for low resource settings, the effect of temperature on the assay performance were tested by detecting rabbit IgGs at ambient temperature (24 °C) and elevated temperature (37 °C). These two conditions represent the temperature range often found in standard laboratories and in the field. The titration data for both types of assays are fitted using a 4-PL (Fig. 5a). The LOD were estimated to be 17.1 ng mL^{-1} and 6.1 ng mL^{-1} for assays performed at 24 °C and 37 °C respectively. This result suggests that an elevated temperature does not have detrimental effect on the performance of the IGSS but rather slightly improves its sensitivity (Fig. 5b).

To characterize the growth of the silver film over time, the IGSS assay was performed using a sample containing a rabbit IgG at a concentration of 4 μg mL^{-1} on microtiter plates and the silver staining process was stopped using three minute intervals. Absorbance measurements taken using a bench-top plate reader are presented in Fig. 5b. The growth of the silver film can be divided into three phases: first, the silver growth exhibits a slow initial phase for approximately 9 min, then the silver staining evolves rapidly between 9 to 21 min. During this time, the thickness of the silver film is proportional to the duration of the silver reduction reaction. After 21 min, the silver staining process reaches plateau, which is typical of electroless plating reactions and in agreement with previously reported data (Hayat 1995).

Next we wanted to investigate if the silver staining method for signal amplification of immune-capture reactions is compatible with capillary-driven microfluidic chips. To this end, we used microfluidic chips with integrated fluorescent microbeads functionalized with anti-rabbit antibodies, samples and solutions of reagents as described earlier. Specifically, a serial dilution of rabbit IgG in 1% BSA in PBS was prepared and such solutions were pipetted on the first loading pad of microfluidic chips and allowed to flow into the chip for 5 min. Each chip was only used once and a fluorescence micrograph around the bead lanes was acquired 7 min after the silver staining solution had been added to the chip. The dependence of the fluorescence attenuation from the beads (microfluidics-based assay) or of the light absorption (microwell-based assay) with the concentration of rabbit IgG in the samples are displayed in Fig. 6 together with some representative images of the silver films and bead lanes. These experiments were performed at RT (24 °C) and in both cases the signal correlates with the concentration of analyte in the sample leading to an increased absorption of light or emitted fluorescence as the concentration of analyte increases. The obtained signals are fitted using a 4-PL and the LOD of the microwell- and microfluidic chip-based assays were found to be 17.1 ng mL^{-1} and 24.6 ng mL^{-1} respectively. Such LODs are very similar and in fact represent an excellent sensitivity considering that polyclonal antibodies were used for this proof-of-concept and that the assay on the microfluidic chip necessitated only 20 min and few microliters of solutions.

4 Conclusion

A microfluidic chip with successful implementation of silver staining and complementary integration of microbeads was developed. The use of fluorescent beads for microfluidics-based immunodiagnostic assays is not a limitation for point-of-care applications because many fluorescence devices have been engineered and fluorescence readers have been developed for various point-of-care applications. The assay with silver staining on chip achieved comparable sensitivity when

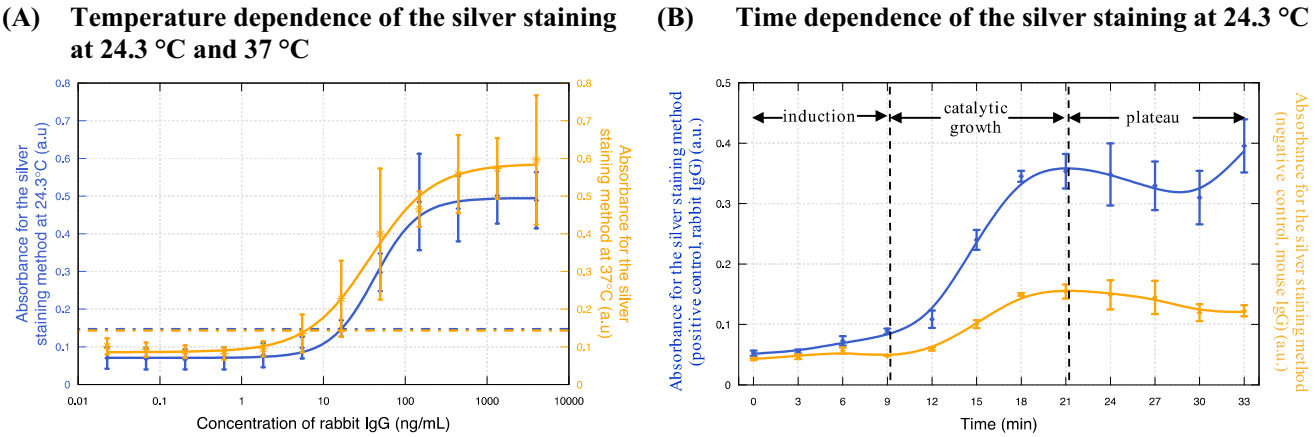

Fig. 5 Kinetics and temperature characteristics of the silver staining reaction in an IGSS assay performed using 96-well microtiter plates. For all experiments, the dilution of gold-conjugated dAb was 1:2000. **a** Comparison of the silver staining step performed at 24.3 °C and 37 °C after 20 min and using optical absorption measurement. **b** The concentration of rabbit IgG in 1% BSA in PBS was 4 μg mL^{-1}. Silver staining was stopped at three minute intervals by addition of deionized water and the optical absorbance of the corresponding silver layer was measured using an UV/Vis plate reader. Standard deviations of triplicate experiments are shown as error bars

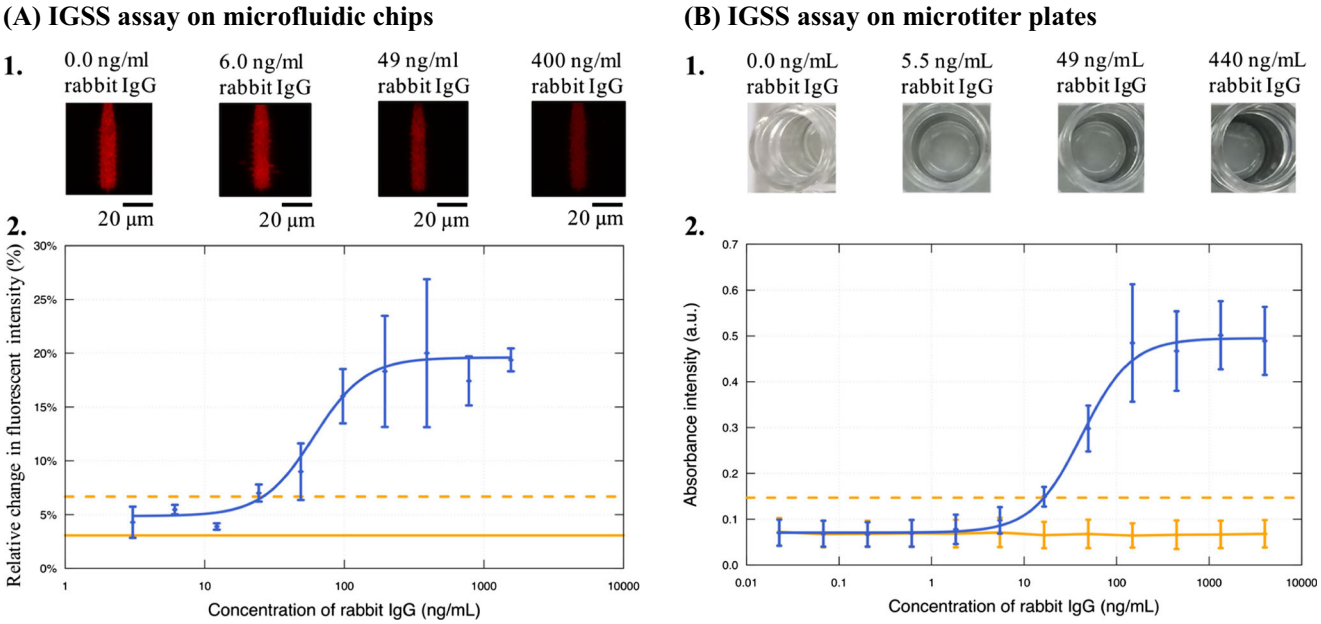

Fig. 6 Performance comparison of the IGSS assays using: (**a**) capillary-driven microfluidic chips and (**b**) 96-well microtiter plates. For all experiments, the dilution of gold-conjugated dAb was 1:2000. **a** 1. Fluorescence micrographs correspond to the attenuation of fluorescence from beads by the stained silver layer after 7 min loading silver mixture. 2. Fluorescence profile of the bead-based IGSS assay on capillary-driven microfluidic chips. The fluorescence images were taken after 7 min flowing of silver mixture on the chip. Standard deviations of triplicates in a single experiment are shown as error bars. Dotted lines represent the cut-off value for this IGSS assay at 24.6 ng mL^{-1}. **b** 1. Photographs of micro-wells correspond to silver staining layers obtained with four different concentrations of rabbit IgG after 20 min. 2. Optical absorbance measurements of the silver layer obtained from IGSS assays performed on 96-well microtiter plates. The absorbance measurements were taken after 20 min incubating with silver mixture then rinsing. Standard deviations of 9 repeats are shown as error bars. Dotted lines represent the cut-off value for this IGSS assay at 17.1 ng mL^{-1}

compared with microtiter plates assays in less than 20 min. Moreover, the implementation of immunogold silver staining in microfluidics system eliminates the need for fully transparent devices when absorption of light is measured, and allows a simple in-plane optical detection system. Effect of temperatures on performance of assays was investigated, presenting no adverse effect for the silver staining immunoassays. While shelf life of reagents and their stability was not investigated in this work, this should not cause any issues since antibodies, commercially-available silver staining solutions and reagents are stable and commonly used for both research and *in vitro* diagnostic applications. The proof-of-concept prototype developed in this work achieves similar performance to that of lab-based immunoassays while retaining most of the advantages of rapid tests. The time taken to carry out an assay is only 20 min and there is no need for active microfluidic elements. Once the liquid is introduced, the flow is self-driven. The chips are designed to be compact and simple to use. Furthermore, the potential for mass production is considered by using dry film resist for easy fabrication, and by utilizing a design on Si that can easily be transferred to available mass production technologies. Possibly, this system can be fully integrated with automatic microfluidic delivery of buffers and reagents. Overall, we demonstrated strategies with which microfluidic chips and microbeads can be combined with silver staining to achieve a performance comparable to a reference lab-based method.

Acknowledgements Ngoc M. Pham is supported through the Engineering for Development doctoral scholarship by ETH Global and the Sawiris Foundation for Social Development. Walter Karlen is supported through the Swiss National Science Foundation professorship award 150640 “Intelligent point-of-care monitoring”. Yuksel Temiz, Robert D. Lovchik and Emmanuel Delamarche thank Elisa Hemmig and Onur Gökçe for discussions and Walter Riess and the IBM Research Frontiers Institute for their continuous support.

References

C.A. Baker, C.T. Duong, A. Grimley, M.G. Roper, Bioanalysis **1**, 967 (2009)

BIO Ventures for Global Health, *The Diagnostics Innovation Map: Medical Diagnostics for the Unmet Needs of the Developing World* (2010)

C.D. Chin, V. Linder, S.K. Sia, Lab Chip **12**, 2118 (2012)

M. A. Hayat (ed.), *Immunogold-Silver Staining: Principles, Methods, and Applications* (CRC Press, Taylor & Francis Group, 1995)

C. Holgate, P. Jackson, P. Cowen, C. Bird, J. Histochem. Cytochem. **31**(7), 938-944 (1983)

H. Gai, Y. Li, E. S. Yeung, Top Curr Chem **304**, 171-201 (2011)

M. Hu, J. Yan, Y. He, H. Lu, L. Weng, S. Song, C. Fan, L. Wang, ACS Nano **4**, 488 (2010)

B. Hu, J. Li, L. Mou, Y. Liu, J. Deng, W. Qian, J. Sun, R. Cha, X. Jiang, Lab Chip **17**, 2225 (2017)

B. Kuswandi, J.H. Nuriman, W. Verboom, Anal. Chim. Acta **601**, 141 (2007)

S.W. Lin, C.H. Chang, C.H. Lin, Genomic Med. Biomarkers, Heal. Sci. **3**, 27 (2011)

R. Liu, Y. Zhang, S. Zhang, W. Qiu, Y. Gao, Appl. Spectrosc. Rev. **49**, 121 (2014)
M. Mirasoli, M. Guardigli, E. Michelini, A. Roda, J. Pharm. Biomed. Anal. **87**, 36 (2014)
P. Novo, D.M. França Prazeres, V. Chu, J.P. Conde, Lab Chip **11**, 4063 (2011)
N. Patel, B.F. Rocks, M.P. Bailey, J. Clin. Pathol. **44**, 334 (1991)
R.W. Peeling, D. Mabey, Clin. Microbiol. Infect. **16**, 1062 (2010)
B.F. Rocks, N. Patel, M.P. Bailey, B. Royaj, S. County, E. Road, Ann. Clin. Biochem. **28**, 155 (1991)
S. Sharma, J. Zapatero-Rodríguez, P. Estrela, R. O'Kennedy, Biosensors **5**, 577 (2015)
I.C. Shekarchi, J.L. Sever, L. Nerurkar, D. Fuccillo, J. Clin. Microbiol. **21**, 92 (1985)
J. Sun, Y. Xianyu, X. Jiang, Chem. Soc. Rev. **43**, 6239 (2014)
Y. Temiz, E. Delamarche, J. Micromech. Microeng. **24**, 97001 (2014)
UNITAID, *Malaria Diagnostics Technology and Market Landscape* (2016), https://unitaid.eu/assets/Malaria_Diagnostics_Technology_and_Market_Landscape_3rd_Edition_April_2016-1.pdf. Accessed 14 May 2018
UNITAID, *HIV Rapid Diagnostics for Self-Testing*, 3rd edn. (2017), https://unitaid.eu/assets/HIV-Rapid-Diagnostic-Tests-for-Self-Testing_Landscape-Report_3rd-edition_July-2017.pdf. Accessed 14 May 2018
A. Wada, Y. Sakoda, T. Oyamada, H. Kida, J. Virol. Methods **178**, 82 (2011)
H. Xu, X. Mao, Q. Zeng, W. Shengfu, A.-N. Kawde, G. Liu, Anal. Chem. **81**, 669 (2009)
P. Yager, T. Edwards, E. Fu, K. Helton, K. Nelson, M.R. Tam, B.H. Weigl, Nature **442**, 412 (2006)
F.Y. Yu, M.M. Vdovenko, J.J. Wang, I.Y. Sakharov, J. Agric. Food Chem. **59**, 809 (2011)